Numerical simulation of hydroelastic waves along a semi-infinite ice floe

Luofeng Huang[1,*], Azam Dolatshah[2,3], Philip Cardiff[4], Luke Bennetts[5], Alessandro Toffoli[3], Zeljko Tukovic[6] and Giles Thomas[1]

[1]*University College London, United Kingdom*
[2]*Swinburne University of Technology, Australia*
[3]*University of Melbourne, Australia*
[4]*University College Dublin, Ireland*
[5]*University of Adelaide, Australia*
[6]*University of Zagreb, Croatia*

Introduction

In the past half century, the effect of global warming has caused the Arctic sea ice thickness to reduce by 50% [1]. The thinned ice vibrates under the excitation from ocean waves, known as its hydroelastic response. Studies on hydroelastic wave-ice interactions started by theoretical models, in which a very long ice floe is usually assumed as semi-infinite and subjected to regular ocean waves. Fox and Squire [2] assumed that the ice floe deforms into a sinusoidal wave-shape, while of a different wavelength and amplitude from the incident waves. By contrast, other authors [3–5] emphasise the hydroelastic waves attenuate with propagation distance and provided predictions of the attenuation. To assess the applicability of these theoretical models, Sree et al. [6] conducted corresponding laboratory experiments using an artificial viscoelastic ice floe and found large discrepancies against the theoretical predictions. Similar inaccuracies of theoretical models were also demonstrated by the experiments of Toffoli et al. [7] and Nelli et al. [8]. With the increasing demand for Arctic Engineering purposes, Squire [9] suggests current theories may have oversimplified the sea ice hydroelasticity, indicating the need to develop numerical models to obtain more realistic solutions.

Numerical models have been reported capable of achieving a full coupling between waves and rigid floating ice [10,11]. When an ice floe is relatively small to wavelength, it is valid for the floe to be considered as rigid, thus no need to solve ice deformations. However, in order to model the sea ice hydroelasticity, a Fluid-Structure Interaction (FSI) approach is required to obtain the structural solution of ice deformation and couple it with the solution of surrounding fluid domain, which requires further development of above models. To fill this gap, an FSI approach [12–16] was developed based on the open-source code, OpenFOAM, and it has been validated in the case of wave interaction with a finite ice floe [17]. In this work, the developed model is extended to a very long ice floe to study the semi-infinite scenario. Simulations are performed to present the wave-induced ice deformation, with the attenuation of hydroelastic waves along the ice floe investigated.

Numerical model

As shown in Figure 1, a two-dimensional rectangular computational domain is established, defined by the Cartesian *xy* coordinate system. To obtain both fluid and structural solutions, the domain is divided into two parts, namely the fluid sub-domain and the solid sub-domain. The domain is 8 m long and 0.6 m high, filled with fresh water of 0.45 m depth, with air filling the rest of the fluid sub-domain. A numerical wavemaker is set at the inlet to generate a regular wave field, propagating in the positive *x*-direction. A range of wave conditions is considered, combined by period T = 0.8 ~ 1.2 s (corresponding to wavelength $\lambda = 1 \sim 2.1$ m) with wave steepness $ka = 0.04 \sim 0.1$. A wave absorption zone is placed by the outlet boundary to minimise reflection of waves. At the top boundary of the domain, a static pressure boundary condition is applied to represent atmospheric conditions. The bottom boundary is defined as a no-slip wall to account for the presence of the seabed. The solid sub-domain represents a high aspect-ratio ice floe floating on the water surface, with length L = 5 m and thickness h = 0.01 m. The ice floe is initialised at its buoyancy-gravity equilibrium position, and its rheology is set at density $\rho = 900$ kg/m^3, Young's modulus E = 4 GPa and Poisson ratio $\nu = 0.4$.

The Finite-Volume method [18] is applied to obtain the fluid and structural solutions over a certain time duration. The process includes two types of discretisation, in space and time respectively. In space, the computational domain is divided into a set of non-overlapping hexahedral cells, known as a mesh; in time, the temporal dimension is split into a finite number of timesteps. As this is an FSI case, the computational mesh is divided into two parts, namely a fluid mesh for the fluid sub-domain and a solid mesh for the solid sub-domain, as depicted in Figure 2. The solutions of the fluid mesh (including velocity, pressure and free surface location) are obtained by

**Presenting author: ucemlhu@ucl.ac.uk*

solving the Navier-Stokes equations incorporating the Volume of Fluid method [17]; the solid mesh is governed by conservation of momentum adopting the nonlinear St. Venant Kirchhoff hyperelastic law [14], so as to capture the ice deformation. The fluid and structural solutions are coupled at the fluid-solid interface, achieved by a Dirichlet-Neumann coupling procedure [13], where velocity and pressure are first calculated in the fluid sub-domain, and the force from the fluid side on the interface is applied as a boundary condition to the solid side of the interface; the displacement in the solid sub-domain is then solved according to the force and the velocity of the solid interface is sent back as a boundary condition to the fluid interface. Iterations are performed over these steps until the interface satisfies the kinematic and dynamic conditions.

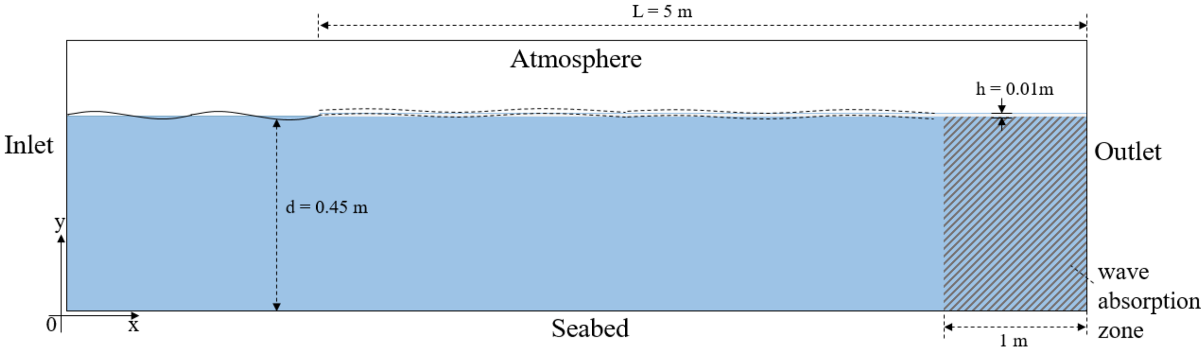

Figure 1: Schematic of the model with dimensions: regular waves propagate in the positive *x*-direction and induce the elastic deformation of a long ice floe floating on the water surface.

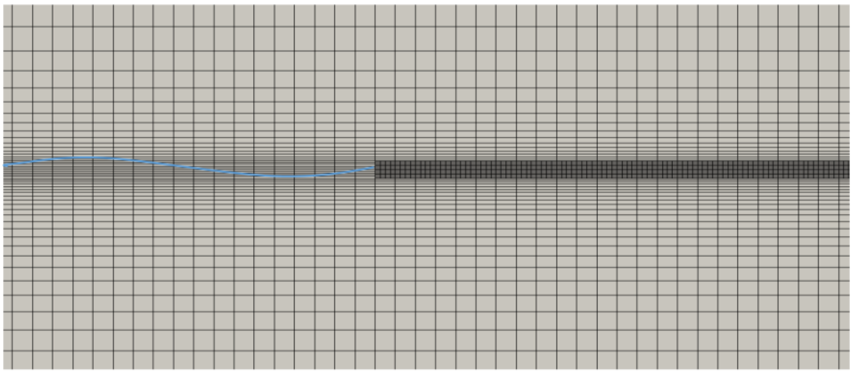

Figure 2: Mesh layout: with fluid mesh (light), solid mesh (dark) and free surface (blue line). The fluid mesh is graded towards the free surface area.

Results and discussion

As shown in Figure 3, with the propagation of waves, the ice floe undergoes vibrations, including sinusoidal oscillations following the wave period and a downward bend due to waves running on top of the ice (referred as overwash [19,20]). The ice deforms into the wave-shape, in which the wave amplitude decreases along the ice, i.e. attenuation, and the wavelength inside the ice is visibly larger than the incident wavelength. Figure 3(a) shows the ice edge bends upwards when a wave crest encounters it. However, it does not show an effective upward displacement, which attributes to the offset of overwash load. Figure 3(b) shows a large downward displacement induced by a wave trough, which has been strengthened by overwash. These suggest the effect of overwash can be a key factor to the hydroelastic ice strain, important for further predicting ice crack and break-up. Overwash is a ubiquitous polar phenomenon due to the very small freeboard of sea ice, which has been reported to be one main gap of current sea ice modelling; its exclusion by previous theoretical models is the primary reason causing inaccuracies [7,8]. Nevertheless, the proposed approach is promising for relevant sea ice predictions since it is fully-coupled with overwash.

To analyse the wave attenuation along the ice floe, vibrations are measured every 0.1 m along the ice floe. An ice vibration amplitude (a_{ice}) is obtained at each measured location, calculated as half the difference between the average peak and trough positions of the oscillation. As shown in Figure 4, for all the tested wave conditions, the amplitude of the ice response decreases as the distance from the ice edge increases, showing the wave energy dissipation due to the viscous effect between water and the ice bottom. Figure 4 (a) presents the attenuation for the same wave steepness but different wave periods. It can be seen that waves of a larger period (or longer waves) can better propagate into the ice. When T = 1.2 s and T = 1 s, an exponential attenuation can be observed. The amplitude decreases from around 95% and 80% of the wave amplitude respectively, and around 35% and 20% can propagate through one meter of the ice. When T = 0.8 s, where the waves are relatively short, the ice edge can only vibrate at around 40% amplitude of the incident wave, and the amplitude quickly reduces to zero after propagating over one meter. For a further location, the vibration is negligible. Figure 4 (b) compares the attenuation at T = 0.8 s but different wave steepnesses, and they all follow the similar trend. For a higher steepness (or higher amplitude), a weaker vibration is obtained, which can attribute to a consequent stronger overwash that can suppress the vibration.

The numerical observations are in accordance with the experiments conducted at the wave-ice tank at the University of Melbourne [21]. Future work will include a numerical and experimental combination to investigate relevant hydroelastic wave-ice interactions. Experimental work can provide valuable insights and validations to support of the development of the numerical model; on the other hand, the numerical method equips convenience to provide cost-effective solutions, attended by the flexibility to investigate the influence of varying environmental variables, e.g. ice dimensions and rheology.

Acknowledgements

This work is part of a project that has received funding from the European Union's Horizon 2020 research and innovation programme under grant agreement No 723526 - SEDNA: Safe maritime operations under extreme conditions; the Arctic case.

(a) t = (n+1/4) T, when a wave crest approaches the ice.

(b) t = (n+3/4) T, when a wave trough approaches the ice.

Figure 3: Deformed ice floe due to waves (T = 1.2 s and *ka* = 0.04); black line indicates its original position.

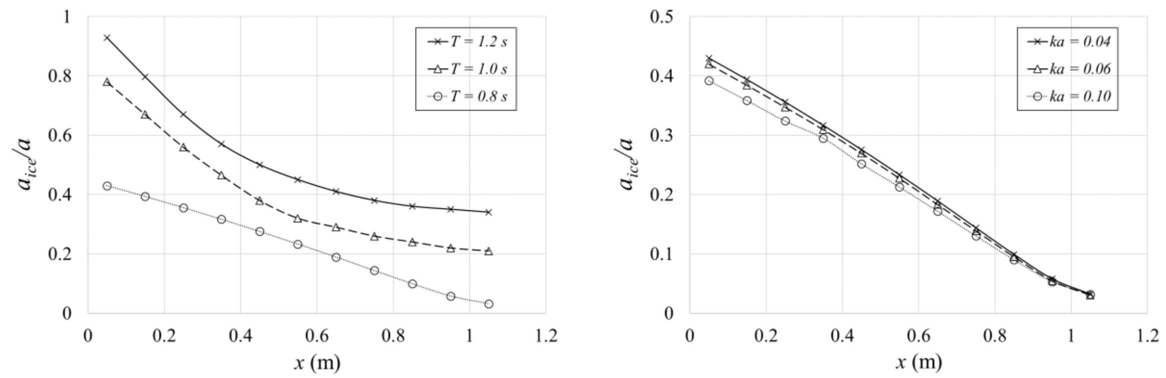

(a) ka = 0.04, with different wave periods

(b) T = 0.8 s, with different wave steepnesses

Figure 4: Non-dimensional vibration amplitude, as a function of horizontal distance from the ice edge.

References

[1] S.W. Laxon, K.A. Giles, A.L. Ridout, D.J. Wingham, R. Willatt, R. Cullen, R. Kwok, A. Schweiger, J. Zhang, C. Haas, CryoSat-2 estimates of Arctic sea ice thickness and volume, Geophys. Res. Lett. 40 (2013) 732–737.

[2] C. Fox, V.A. Squire, On the oblique reflexion and transmission of ocean waves at shore fast sea ice, Phil Trans R Soc Lond A. 347 (1994) 185–218.

[3] V.A. Squire, A. Allan, Propagation of flexural gravity waves in sea ice, Centre for Cold Ocean Resources Engineering, Memorial University of Newfoundland, 1977.

[4] N.J. Robinson, S.C. Palmer, A modal analysis of a rectangular plate floating on an incompressible liquid, J. Sound Vib. 142 (1990) 453–460.

[5] R. Wang, H.H. Shen, Gravity waves propagating into an ice-covered ocean: A viscoelastic model, J. Geophys. Res. Oceans. 115 (2010).

[6] D.K. Sree, A.W.-K. Law, H.H. Shen, An experimental study on gravity waves through a floating viscoelastic cover, Cold Reg. Sci. Technol. 155 (2018) 289–299.

[7] A. Toffoli, L.G. Bennetts, M.H. Meylan, C. Cavaliere, A. Alberello, J. Elsnab, J.P. Monty, Sea ice floes dissipate the energy of steep ocean waves, Geophys. Res. Lett. 42 (2015) 8547–8554.

[8] F. Nelli, L.G. Bennetts, D.M. Skene, J.P. Monty, J.H. Lee, M.H. Meylan, A. Toffoli, Reflection and transmission of regular water waves by a thin, floating plate, Wave Motion. 70 (2017) 209–221.

[9] V.A. Squire, Past, present and impendent hydroelastic challenges in the polar and subpolar seas, Philos. Transact. A Math. Phys. Eng. Sci. 369 (2011) 2813–2831. doi:10.1098/rsta.2011.0093.

[10] W. Bai, T. Zhang, D.J. McGovern, Response of small sea ice floes in regular waves: A comparison of numerical and experimental results, Ocean Eng. 129 (2017) 495–506.

[11] L. Huang, G. Thomas, Simulation of Wave Interaction with a Circular Ice Floe, J. Offshore Mech. Arct. Eng. (2018). doi:10.1115/1.4042096.

[12] Z. Tukovic, H. Jasak, Updated Lagrangian finite volume solver for large deformation dynamic response of elastic body, Trans. FAMENA. 31 (2007) 55.

[13] Ž. Tuković, A. Karač, P. Cardiff, H. Jasak, A. Ivanković, OpenFOAM Finite Volume Solver for Fluid-Solid Interaction, Trans. FAMENA. 42 (2018) 1–31. doi:10.21278/TOF.42301.

[14] P. Cardiff, A. Karač, P. De Jaeger, H. Jasak, J. Nagy, A. Ivanković, Ž. Tuković, An open-source finite volume toolbox for solid mechanics and fluid-solid interaction simulations, ArXiv Prepr. ArXiv180810736. (2018).

[15] L. Huang, An opensource solver for wave-induced FSI problems, Proc. CFD OpenSource Softw. Ed. Nilsson H. (2018). doi:http://dx.doi.org/10.17196/OS_CFD#YEAR_2017.

[16] L. Huang, M. Li, Z. Tukovic, G. Thomas, Simulation of the hydroelastic response of a floating ice sheet, 13th OpenFOAM Workshop. (2018).

[17] L. Huang, K. Ren, M. Li, Ž. Tuković, P. Cardiff, G. Thomas, Fluid-structure interaction of a large ice sheet in waves, ArXiv Prepr. ArXiv181203493. (2018).

[18] H.K. Versteeg, W. Malalasekera, An introduction to computational fluid dynamics: the finite volume method, Pearson Education, 2007.

[19] D.M. Skene, L.G. Bennetts, M.H. Meylan, A. Toffoli, Modelling water wave overwash of a thin floating plate, J. Fluid Mech. 777 (2015).

[20] D.M. Skene, L.G. Bennetts, M. Wright, M.H. Meylan, K.J. Maki, Water wave overwash of a step, J. Fluid Mech. 839 (2018) 293–312.

[21] A. Dolatshah, F. Nelli, L.G. Bennetts, A. Alberello, M.H. Meylan, J.P. Monty, A. Toffoli, Hydroelastic interactions between water waves and floating freshwater ice, Phys. Fluids. 30 (2018) 091702.